



Application of Electric Field to Developing Falling Films using Wire-Plate Electrode Configuration- An Experimental Study

R. Rouhollahi¹, S. Baheri Islami^{1†}, R. Gharraei² and M. R. Heirani Nobari³

¹ Faculty of Mechanical Engineering, Department of Mechanical Engineering, University of Tabriz, Tabriz, Iran

² Mechanical Engineering Department, Azarbaijan Shahid Madani University, Tabriz, Iran

³ Department of Mechanical Engineering, Amirkabir University of Technology, Tehran, Iran

†Corresponding Author Email: baheri@tabrizu.ac.ir

(Received January 5, 2018; accepted April 15, 2018)

ABSTRACT

Experimental investigation of Electrohydrodynamic developing film flow of transformer oil has been conducted within an inclined rectangular channel and hydrodynamic characteristics of the flow have been revealed. The electric field has been generated by five overhead thin wire electrodes connected to the positive high DC voltage on the air and the grounded plate electrodes which are placed upon the floor of the channel. It is the first time that the wavy behavior on a liquid falling film's interface has been created by this electrode configuration. A non-intrusive method has been used to measure the local flow structure by a high-speed camera, then statistical characteristics of the wavy falling film have been computed by image processing of the captured video frames. By applying 13-16 kV to the wire electrodes, the influence of EHD force on the wavy behavior of falling film has been conducted for Reynolds number 10-120 in the laminar-wavy regime at three different inclination angles 15°, 30° and 45°. The vertical distance of the high-voltage wire electrodes to ground electrodes has been set to 14 mm. The liquid velocity, film thickness, and wave frequency have been measured for non-electrified and electrified falling film, and their results have been evaluated with other experimental studies and an acceptable agreement has been obtained. The results indicate that the proposed HV wire-grounded plate electrode configuration in this study does not disturb the original structure of the falling film and by intensifying the wavy behavior of laminar falling film can either suppress or enhance heat/mass transfer rate. The effects of the applied voltage on the frequency, velocity and film thickness of the falling liquid film have been also discussed in detail.

Keywords: EHD; Falling film; Dielectric; Image processing; Wire-plate electrode.

NOMENCLATURE

\vec{E}	electric field strength	V	voltage
\vec{F}_e	electric force	w	channel width
f	frequency	δ	film thickness
g	gravity acceleration	ε	fluid permittivity
Q	volumetric flow rate	θ	inclination angle
q_c	free electric charge density	ν	kinematic viscosity of fluid
p	pressure	σ_e	electrical conductivity
Re	Reynolds number	τ	time
S	standard deviation	M	maxwell
T	temperature	Max	maximum
t	time	Nu	nusselt
u	velocity	*	dimensionless

1. INTRODUCTION

Because of widespread utilization of falling films

on inclined surfaces in industrial application where heat and mass transfer take place, many studies have been done in the last 50 years in order to

design a reliable type of equipment and accurate prediction of heat/mass rates (Moran, Inumaru, and Kawaji 2002), (Drosos, Paras, and Karabelas 2004). Extensive theoretical and experimental investigations have been observed that the interfacial and wall-to-liquid heat/mass transfer is highly dependent on the waviness of the gas-liquid interface, in particular, and variation of hydrodynamic characteristics like film thickness, velocity, and frequency (Ambrosini *et al.* 1999; Charogiannis, An, and Markides 2015; Tseluiko and Papageorgiou 2006).

Applying an intense electric field to augment heat transfer has been continuously investigated over the past 80 years. Most of the early works have been focused on the single-phase flows' enhancement. Many researchers, over the last 30 years, have pointed out that in two-phase flows, EHD has a great potential to enhance heat transfer by destabilizing the liquid film along the walls. In Electrohydrodynamic methods used to enhance of the heat transfer, an electric field is coupled with a dielectric medium (Chirkov 2013; Gonzalez and Castellanos 1996; Laohalertdecha, Naphon, and Wongwises 2007). To date, in order to explain the observed EHD phenomena, several mechanisms have been proposed, namely, ion injection, conduction pumping and induction pumping (Raghavan *et al.* 2009). In this technique, a high-voltage electric field with low-current either DC or AC is applied through the dielectric medium which is flowing between high-voltage and grounded electrodes. In an EHD flow, the electric field energy is directly transformed into the fluid's kinetic energy. Wide application of EHD flows can be observed in modern knowledge-intensive technologies, and EHD pumps, heat exchangers, atomizers, and filters are some of EHD-based device (Chirkov 2013; Laohalertdecha, Naphon, and Wongwises 2007). Some of the advantages of EHD enhancement are (Seyed-Yagoobi and Bryan 1999):

- (a) Altering the electric voltage to control the enhancement rate smartly and quickly.
- (b) Simple design without mechanical parts.
- (c) Compatible with space environment's applications.
- (d) Presumable to single-phase and multiphase flows.
- (e) Low power expenses.

EHD can be applied to enhance the heat transfer of the condensation by inducing perturbations and waviness into the condensate film (Molki, Ohadi, and W. Da Silva 2002; Seyed-Yagoobi and Bryan 1999; Wang *et al.* 2009). Furthermore, the boiling process can be augmented by EHD techniques through creating more waves and perturbations at the boiling liquid's surface (Damianidis, Karayiannis, and Al-Dadah 1992; Ogata and Yabe 1993; Wang *et al.* 2009). When a high voltage applied to a fine wire or a sharp needle, air will be ionized in its vicinity and above a body of liquid,

and the electrically grounded plates will attract these ions. During the movement to the plate electrodes, the ions collides with neutral molecules and momentum transfer occurs between them. This bulk flow of ionized air molecules is known as Corona wind which by disturbing the boundary layer on the grounded surface, can enhance heat/mass transfer between the air and grounded surface (Molki, Ohadi, and W. Da Silva 2002; Seyed-Yagoobi and Bryan 1999). Karami *et al.* revealed by an experimental study that the level of the evaporation enhancement could be achieved by Corona wind in the wind tunnel (Karami *et al.* 2012). The Corona wind velocity, electrode spacing, and air flow's velocity were examined in order to assign their effect on the evaporation enhancement. Ohyama *et al.* conducted an experiment to study current conduction phenomenon and EHD induced flow for the air-wave type EHD pump with a gas-phase wire electrode and a plate electrode parallel to the gas-liquid interface (Ohyama, Watson, and Chang 2001). They observed that significant waves appeared on the interface of the liquid, which flows over the plate electrode due to EHD instability. Also, by increasing the voltage, the thickness of the liquid layer and the interfacial liquid velocity increased. Nourdanesh and Esmailzadeh investigated experimentally the conduction pumping in different liquid temperature and film thicknesses in order to find the optimum film thickness to enhance the heat transfer coefficient. They also studied the volume flow rate, heat transfer per power consumption and efficiency of free surface liquid film (Nourdanesh and Esmailzadeh 2013). Experimental study of the developing falling film was done by Gharraei *et al.* due to determine the hydrodynamic behavior of the film when the EHD conduction phenomenon is imposed (Gharraei *et al.* 2015). Their measurements represented that the instabilities and wavy behavior of developing falling film flow will be intensified by applying the electric field. The fully developed flow of falling film was investigated experimentally by (Sobhani *et al.* 2015) in the presence of conduction pumps. Results indicated that the thickness of falling film would decrease by applying electric field in a wide range of Re numbers. It was also presented the behavior of wave's frequency and velocity with respect to Re number for each arrangement. The wave's frequency in conduction pumps was increased at low Reynolds numbers while conversely decreased at high ones.

In most studies, application of electric field on falling film leads to the phase change that alters the original structure of the film. It appears from the reviews that very little work has been done so far on electrified falling films without distortion of their structure. For example, Gonzalez and Castellanos produced an electric field by two parallel plates, which imposed normally to the flow direction and in which ground electrode was placed far from the film surface (Gonzalez and Castellanos 1996). It was observed that an intense electric field normal to film flow direction would induce instability to the

film. The instability of falling films in the presence of normal exerted electric field on the flow has also been investigated in (Gonzalez and Castellanos 1996), (Samanta 2013; Tseluiko *et al.* 2010; Wray, Matar, and Papageorgiou 2012).

The present study is concerned with a new type of EHD phenomenon on the falling film flow of a dielectric liquid using thin wire high voltage electrodes in a gas phase similar to the induction pumps and ground electrodes in the liquid phase parallel to the wires like to conduction pumps. In this work, a dielectric liquid has been actuated without having contact with the high-voltage electrodes. Therefore, despite other EHD mechanisms, this electrode system can operate with weak dielectric liquids. In this mechanism, the surface charge is induced in the dielectric liquid interface due to existence of the permittivity gradient across it. Due to the absence of charge injection into the liquid and the ion dissociation in this suggested EHD mechanism, dielectric property of the liquid will not change and general flow structure of falling film will not alter (Raghavan *et al.* 2009). The effect of plate inclination and applied voltage on the liquid film thickness, flow velocity, and wave frequency has been discussed in detail. Additional information on maximum and substrate film thickness, standard deviation, PDF, and power spectral density function are also presented. Intensifying wavy structures in the liquid film flow is the motivation behind this study for enhance the heat/mass transfer exposed to an electric field.

2. ELECTROHYDRODYNAMIC FORCES

Electrohydrodynamics (EHD) is interpreted as an interplay between an electric field and fluid flow. The imposed electric body force on the fluid consists of three terms, which can be declared by the Korteweg–Helmholtz equation (Léal *et al.* 2013):

$$\vec{F}_e = q_c \vec{E} - \frac{1}{2} E^2 \vec{\nabla} \varepsilon + \frac{1}{2} \vec{\nabla} \left(\rho E^2 \left[\frac{\partial \varepsilon}{\partial \rho} \right]_T \right) \quad (1)$$

The first term in Eq. (1) represent the coulombic force (or electrophoretic force) imposed on free charges in the liquid. When there is net charge in the dielectric fluid, this electrostatic force is induced. The ionic wind (ionic flow of charged particles) is caused due to this Coulomb force, which plays a significant role in heat transfer enhancement in a single phase. Indeed, the presence of thermal gradients within the fluid of single-phase leads to non-uniformity in electrical conductivity σ_e and in dielectric permittivity ε . The polarizability of the dielectric fluid is characterized by the permittivity (Léal *et al.* 2013). The second term (dielectrophoretic force) stands for a dielectric force induced by permittivity gradient. For example, the required permittivity gradient can be generated by the presence of a liquid/vapor or liquid/liquid interface, the existence of non-isothermal conditions or electrical inhomogeneity in a single-phase liquid. The third term pointed out to electrostriction effect which can happen in

compressible fluid (Raghavan *et al.* 2009). The above equations coupled with the conservation equations are solved to determine the fluid flow and temperature fields (Seyed-Yagoobi and Bryan 1999).

When a potential difference is applied to parallel electrodes, an electric field appears between them. Electric force in the dielectric liquid can arise from free charges ($q_c \vec{E}$) and from polarization charges ($-1/2 E^2 \vec{\nabla} \varepsilon$). It is evident that the permittivity does not vary within the isothermal liquid, so the polarization force in the bulk is zero. Therefore, there are no electrical forces in the bulk of liquid and the electromechanical coupling takes place at the interface, where there are both free and polarization charges (Melcher 1966). In this experiment, the HV wire electrodes are not in contact with the liquid, but they apply force on the free liquid surface. Due to the interaction between induced charges, the normal electric field across the interface and normal gravitational forces an attraction force will be created, which draws the fluid of higher permittivity (liquid) towards the region of higher electric field strength and the waves are generated at the liquid surface as shown in Fig. 1. If there is a potential accumulation of charge on the interface, the polarization force can be affected. Locally, when the charge accumulation is significant, the Coulomb force can be influential (Seyed-Yagoobi and Bryan 1999). On the other hand, if the tangential gravitational and viscous forces and tangential component of electric force are balanced at the interface, there will be an interfacial tangential shear (Raghavan *et al.* 2009), (Paillat and Touchard 2009).

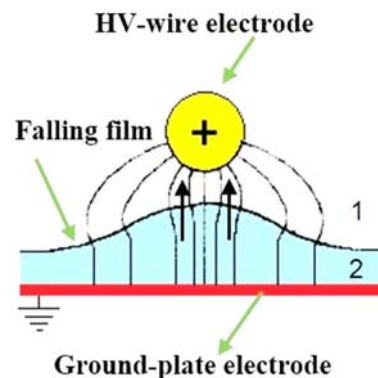


Fig. 1. Simple representation of electric body force components ($\varepsilon_1 > \varepsilon_2$) (Seyed-Yagoobi and Bryan 1999)

3 .EXPERIMENTAL APPARATUS AND METHODOLOGY

A closed-loop experimental set-up is constructed to investigate the behavior of a liquid falling film in an inclined configuration (Fig. 2). The main object of this study is measuring the wave characteristics in falling liquid films because of the close relation between the waviness and heat/mass transfer rate enhancement. A dielectric liquid film flows down a rectangular Plexiglas plate in order to facilitate

visual observations. The channel has 1800 mm length and 160 mm width mounted on a metallic frame. The plate inclination angle θ is adjustable by rotation of the mounting frame around an axis to analyze the behavior of liquid film at 15°, 30° and 45° angles with respect to the horizon. Details of the schematic view of experimental set-up shown in Fig. 2 are presented in (Gharraei *et al.* 2015). We used a high-speed camera to observe the flow pattern that its capturing speed is the 240 frame per second. Whole of the set-up has been located in a dark room for the better fluid film thickness visualization. The liquid-air interface is illuminated with a light sheet generated by SMD lamps. At each Reynolds number ($Re = 4Q/vw$), record time of videos is considered 2.5 second. The camera is directed to the second, third and fourth pairs of the electrodes, which capture the film interface for studying the behavior of falling film. The recorded movies in “.MOV” format has been transferred into a computer to analyze separated frames by image processing codes in MATLAB. This code converts each frame into “HSI” field and can distinguish the illuminated interface from dark surrounding by finding the highest intensity in each column of the image matrices in MATLAB.

The film mean thickness is determined by averaging the liquid film thicknesses in the frames. The statistical methods are also applied to obtain the wave's frequency and velocity by which have been fully explained by Gharraei (Gharraei 2011). Details of the test-section geometry are shown in Fig. 3. Five ground flush mounted electrodes made of copper plates of 5 mm thickness with 16 mm width have been installed on the channel floor as shown in Fig. 3(a). The ground electrodes are spaced evenly over the plate length at a distance of 18 mm. Five high-voltage wire electrodes made of copper with 1 mm outside diameter are horizontally placed perpendicular with the channel axis over the air-liquid interface as shown in Fig. 3(b). To ensure that the test-section is insulated electrically, special high-voltage wires, which are able to work on voltages about 16 kV, have been used. The vertical HV-ground distance is set to 14 mm. According to (Ohyama, Watson, and Chang 2001), HV-ground distance is selected 14 mm that is higher than 10 mm to avoid bridge forming. The wire electrodes are connected to a positive polarity DC high-voltage power supply. Onset of the electric field effect on the falling film occurs at 13 kV for all the cases, and no significant effect has been obtained below 13 kV. For voltages exceeding 16 KV, discharge between HV electrode and interface occurs.

The distance of first ground electrode from film entry is considered 150 mm because wave inception distance for various degrees of inclination and $Re < 120$ is lower than 200 mm according to (Brauner and Maron 1982). The channel is carefully leveled in each angle because of the sensitivity of the longitudinal flow development to geometrical deficiency. The Plexiglas's inner surface of the test section is cleaned by a dilute detergent solution before each experiment and dried by an air flow. In this study, the film Reynolds number ranges from 10

to 120. It should be mentioned that waves in the test section, for all range of Reynolds number, are two-dimensional. This 2-D shape observed for $Re < 15$ up to the lower part of the inclined plate and time-average film thickness distribution over the plate is flat. When the Reynolds number is increased, the transition to the three-dimensional wave regime occurs in the bottom of the plate (Bobylev *et al.* 2016). Transformer oil is used as working fluid and its physical and electrical properties are presented at the ambient temperature (25°C) in Table. 1.

4. STATISTICAL QUANTITIES AND MATHEMATICAL FORMULATIONS

The instantaneous non-electrified and electrified film thickness $\delta(t)$ is supposed to be a random fluctuating quantity. Using, the following statistical parameters can be calculated from the time-series analysis on the data: mean film thickness, δ_{mean} , probability density function (PDF), auto-correlation function, cross-covariance function and spectral density function. To calculate these parameters, 5000 samples have been used which are obtained over a period of 2.5 seconds with a sampling frequency of 240 Hz. The mean film thickness is calculated by averaging N instantaneous film thickness, δ_i , for each data set (Moran, Inumaru, and Kawaji 2002),

$$\delta_{mean} = \frac{\sum_{i=1}^N \delta_i}{N} \quad (2)$$

The one-dimensional, steady, fully developed gravity-driven film flow solution proposed by Nusselt is used to compare with the experimental mean film thickness (Lel *et al.* 2005):

$$\delta_{Nu} = \left(\frac{3\nu^2 Re}{4g \sin \theta} \right)^{\frac{1}{3}} \quad (3)$$

In order to compare the data of the present work with other results in the literature, film thickness has been reported in the dimensionless form defined by (Lel *et al.* 2005):

$$\delta^* = \delta \left[\frac{g \sin \theta}{\nu^2} \right]^{\frac{1}{3}} \quad (4)$$

In order to obtain wave velocity data for falling film, a method based on the discrete cross-covariance function has been used to the recorded film thickness. In this method, the instantaneous film thickness data at two positions of the plate by separation distance L_{sep} is considered to calculate the average time shift, τ^* , between these series as follows (Ambrosini *et al.* 1999):

$$C_{12,k} = \frac{1}{N} \sum_{i=0}^{N-1} (\delta_1(t_i) - \bar{\delta}_1)(\delta_2(t_i + \tau_k) - \bar{\delta}_2) \quad (5)$$

where $t_i = i.\Delta t$ and $\tau_k = k.\Delta t$ and Δt is the effective sampling period (which is equal to 0.00416 s in this study). By plotting the calculated C_{12} versus time and finding the maximum amplitude of the curve, the corresponding average time shift, τ^* , between two points is obtained. By known separation distance of $L_{sep} (= 17 \text{ mm}$ in our case), the average wave velocity is determined by the following equation (Ambrosini *et al.* 1999):

- 1.Lower Storage Tank
- 2.Liquid Pump
- 3.Controller Valve
- 4.Controller Valve
- 5.Upper Storage Tank
- 6.Controller Valve
- 7.Constant Head Tank
- 8.Gate Valve
- 9.Controller Valve
- 10.Reservoir Tank
- 11.Measuring Tank
- 12.Controller Valve
- 13.DC High Voltage Source
- 14.High Voltage Wire
- 15.Ground Wire
- 16.High-speed Camera
- 17.SMD lump

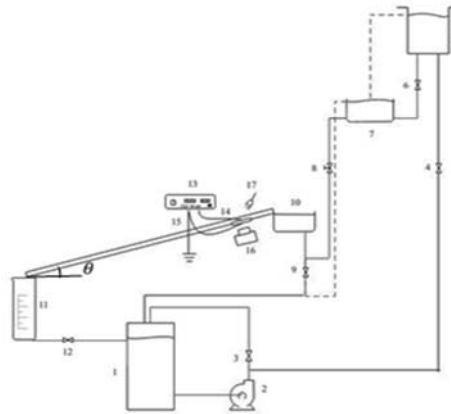


Fig. 2. Schematic diagram of experimental set-up

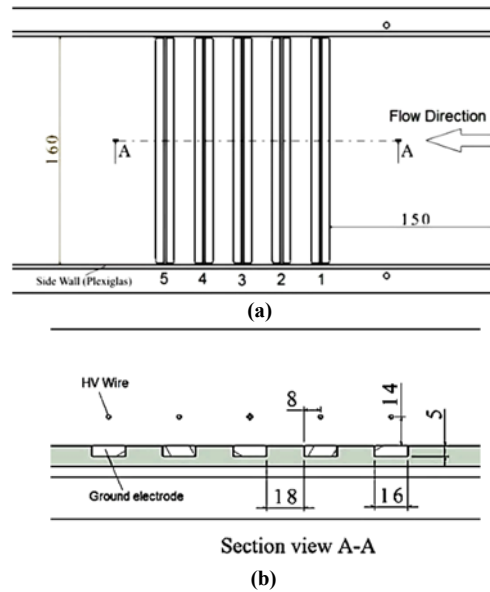


Fig. 3. Schematic view of (a) test-section, (b) Details of electrodes arrangement (Dimensions in mm)

$$u_w = \frac{L_{sep}}{\tau^*} \quad (6)$$

The average wave velocity predicted by Nusselt along the stream-wise direction to the flow can be calculated from Eq. (7) which extracted by integrating the velocity profile across the film thickness (Portalski 1964).

$$\bar{u}_{Nu} = \frac{\delta^2 g \sin \theta}{3\nu} \quad (7)$$

The wave velocity is presented in term of a dimensionless parameter in order to compare them with data reported throughout the literature for different conditions:

$$u^* = \frac{u_w}{(\nu g \sin \theta)^{1/3}} \quad (8)$$

The frequency composition of the wave can be determined by calculating power spectral density of the local instantaneous film thickness. Power spectral density of the waves is obtained by applying a Fourier transform utilizing the Welch algorithm on the fluid thickness varying with time

at one spatial location (Martin *et al.* 2015). A Hamming window function is applied to decline the spectral leakage while carrying out the Fourier transform (Ambrosini *et al.* 1999). The frequency corresponding to the maximum magnitude of PSD for instantaneous film thickness at a defined distance from the entry is determined as wave frequency characteristics, f may be related with the frequency of the large wave, while the weaker peaks are likely to represent smaller waves developing on the substrate between large waves. The non-dimensional frequency has been defined as (Miyara 1999):

$$f^* = \frac{f \delta_{Nu}}{\bar{u}_{Nu}} \quad (9)$$

Probability density function (PDF) of instantaneous film thickness data is used to evaluate the substrate thickness and the effect of EHD on it. In this work, 0.1 mm interval is considered to calculate PDF of film thickness and study the film waviness at different Reynolds number and voltages. The main peak indicates the most probable film thickness, which can be considered to represent the substrate

film thickness, and the additional peaks at greater film thickness values correspond to the small and large amplitude waves (Moran, Inumaru, and Kawaji 2002). If F_δ was the probability of the occurrence of thickness lower than δ , PDF could be defined as (Chu and Dukler 1974):

$$F_\delta = Prob(\delta(t) < \delta) \quad (10)$$

$$PDF = \frac{dF_\delta}{d\delta} \quad (11)$$

The standard deviation of the instantaneous film thickness represents a way to evaluate the fluctuations around the mean film thickness. In this regard, it can also represent the waviness of the gas-liquid interface. This quantity is the positive square root of the second central moment which is defined as (Moran 1997):

$$S = \left\{ \lim_{T \rightarrow \infty} \frac{1}{T} \int_T [\delta(t) - \bar{\delta}]^2 dt \right\}^{\frac{1}{2}} \quad (12)$$

5. RESULTS

Experiments have been performed at 25°C and 10 different volumetric flow rates (Q) and Reynolds number 10-120. We have conducted the uncertainty analysis conducted according to the method of Moffat (Moffat 1988). The uncertainty of the film thickness and frequency is calculated based on the calibration of captured frames, which are directly correlated with Reynolds number and applied voltage. Therefore, uncertainty of these parameters will have the larger values at high Re numbers. Similarly, the uncertainty will increase with applied voltages. The accuracy of thickness, time and voltage measurement have been estimated about 0.031mm, 0.0042s and 0.1kV, respectively. The

maximum uncertainty of film thickness measurement is calculated about 3.35%.

Figure 4 shows the dimensionless mean film thickness of the non-electrified falling film with various inclination angles in comparison with other reported data due to verify the results of the current experimental study. It is observed that the results of the present study are in good agreement with Brauer (Brauer 1956), Jackson (Jackson 1955) and Nusselt's prediction (Nusselt 1916), while Karapantsios *et al.* (Karapantsios, Paras, and Karabelas 1989) mean film thickness data are smaller than Nusselt's theory and other predictions. There is a high scattering of data because each study involved various working fluids, experimental conditions (developed flow) and distinct measuring techniques.

The non-dimensional wave frequency data derived from image processing at 243 mm downstream (middle of third and fourth HV wire electrode from the entry, have been compared with other available experimental results in Fig. 5. This figure shows that the dimensionless wave frequencies are in good agreement with (Moran, Inumaru, and Kawaji 2002) which were measured in the fully developed region and Jones & Whitaker (Jones and Whitaker 1966) which were measured in the developing region on a vertical plate.

In general, the increase of the Reynolds number causes the wave inception occurs in a greater distance of entry (Brauner and Maron 1982) that depending on the measuring region (developing or fully developed region), can lead to the increase or decrease the wave frequency. On the other hand, reducing the inclination results in wave incepts at greater distance from entry.

Table 1 Physical and electrical properties of transformer oil (25°C).

Density (kg/m ³)	Viscosity (10 ⁻⁵ m ² /s)	Electrical conductivity (10 ⁻¹⁰ S/m)	Dielectric constant
ISO 3675	ASTM D 445	ASTM 24-82b(1982)	ASTM D1169-89(1989a)
864	1.85	1.6	3.4

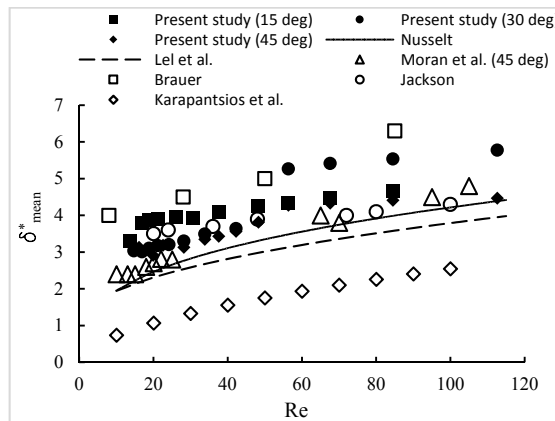


Fig. 4. Comparison of dimensionless film thickness with other experimental studies

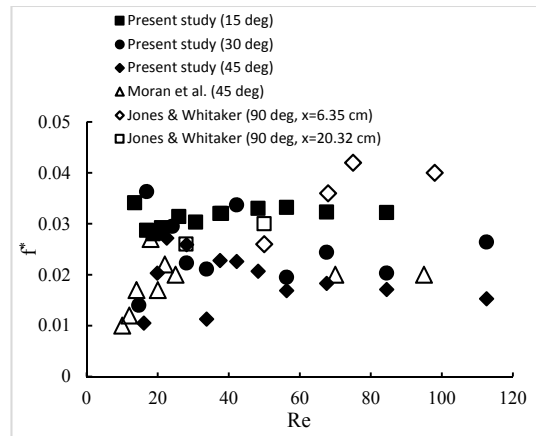


Fig. 5. Comparison of dimensionless wave frequency taken from this study and other experimental data

According to the mathematical relation between frequency, Reynolds number and inclination angle mentioned in section (4), it's expected that the wave frequency decreases by increasing the inclination, and the wave frequency increases slightly by increasing the Reynolds number for all inclination angles, which are consistent with Fig. 6. It is worthwhile to mention that the power spectral density (PSD) diagram shows that most of the wave energy is carried by waves with frequencies less than 6 Hz. As expected, the mean film thickness data and wave frequencies agree generally with other literature data and so, the used measurement techniques are acceptable.

Figure 6 illustrates the formation of large waves on the liquid interface flowing between HV-wire and ground electrodes at voltage 15 kV to compare with non-electrified to show the effect of electric field on the film thickness at inclination angle 30° for low and high Reynolds numbers. When a high voltage is applied to the electrodes, large waves are generated at the liquid surface. In the present experiment, the presence of permittivity gradient in the liquid/air interface leads to normal di-electrophoretic force from high permittivity liquid toward low permittivity air. The interaction between gravitational and electrical body forces causes the formation of such large waves on the surface of falling film. It is noteworthy that the gravitational body force manages the net flow, but the electric force affects the shape of waves and flow's mean thickness.

When a high-intensity electric field applied between an HV wire electrode and a flat plate ground electrode, air molecules near the high-voltage wire discharge region become ionized. The ionization zone exists in the close proximity to the wire electrode, and positive free charges generated. The outside region of the ionization zone possesses single polarity charges that the electric field has drawn them out of the ionization region. When the radius of the HV wire electrode is much smaller than HV-ground distance, the ionization zone forms a uniform sheath over the HV electrode surface.

By traveling the ionized air molecules towards the grounded electrode, collision with air molecules occurs. During this collision, momentum transfers

from the ionized air molecules to neutral ones. Now, when a dielectric liquid is flowing between the HV wires and ground electrodes, the charged liquid free surface moves over the plate ground electrode, and the surface waves formed by interaction between electrostatic forces on the charged surface due to the low conductivity of the liquid, viscous and gravitational forces (Ohyama, Watson, and Chang 2001). Increasing the applied voltage intensifies the growth of the waves on the interface of the film. A properly detailed analysis requires numerical study of the generated electric field. Ground electrodes are depicted by white rectangles and high-voltage wires are placed in the middle of ground electrodes at a fixed height, which their number is shown below each electrode in Fig. 6(a). By comparing Figs. 6(b) and (c) for two successive times, it is observed that the steady profile waves formed at the falling film surface for low Reynolds number in the presence of electric field. These waves for high flow rates, as shown in Figs. 6(d)-(j), are not steady and because of acceleration of flow, coalescence of waves makes the wave height and maximum thickness of film to increase but the number of waves at the liquid film interface is reduced. Therefore, as it is obvious in Figs. 6(b) and (e), the wavelength will rise by the increase of Reynolds number but the wave frequency increases slightly with the increase of Re number. It is obvious that peak of the waves appears away from the HV-wires conjunction with ground electrodes. Due to the gravitational waves, the distance between wave's peak and HV-wire increases with Reynolds number. It should be noted that by increasing the voltage, the charge density at the liquid interface increases. On the other hand, the film interface distance to HV wire will reduce due to the increase of applied force on the liquid interface and produce a discharge between HV wires and interface (plays as a ground) in the form of spark (as shown in Fig. 7). In other words, if the voltage applied to air (as an insulation) progressively increases, there will finally take place a breakdown of the insulation, and a short circuit between the electrodes generates during a breakdown. The breakdown voltage of insulation depends upon the distance between the electrodes, thickness of the liquid and air gap (Seyed-Yagoobi and Bryan 1999), (Tareev 1975).

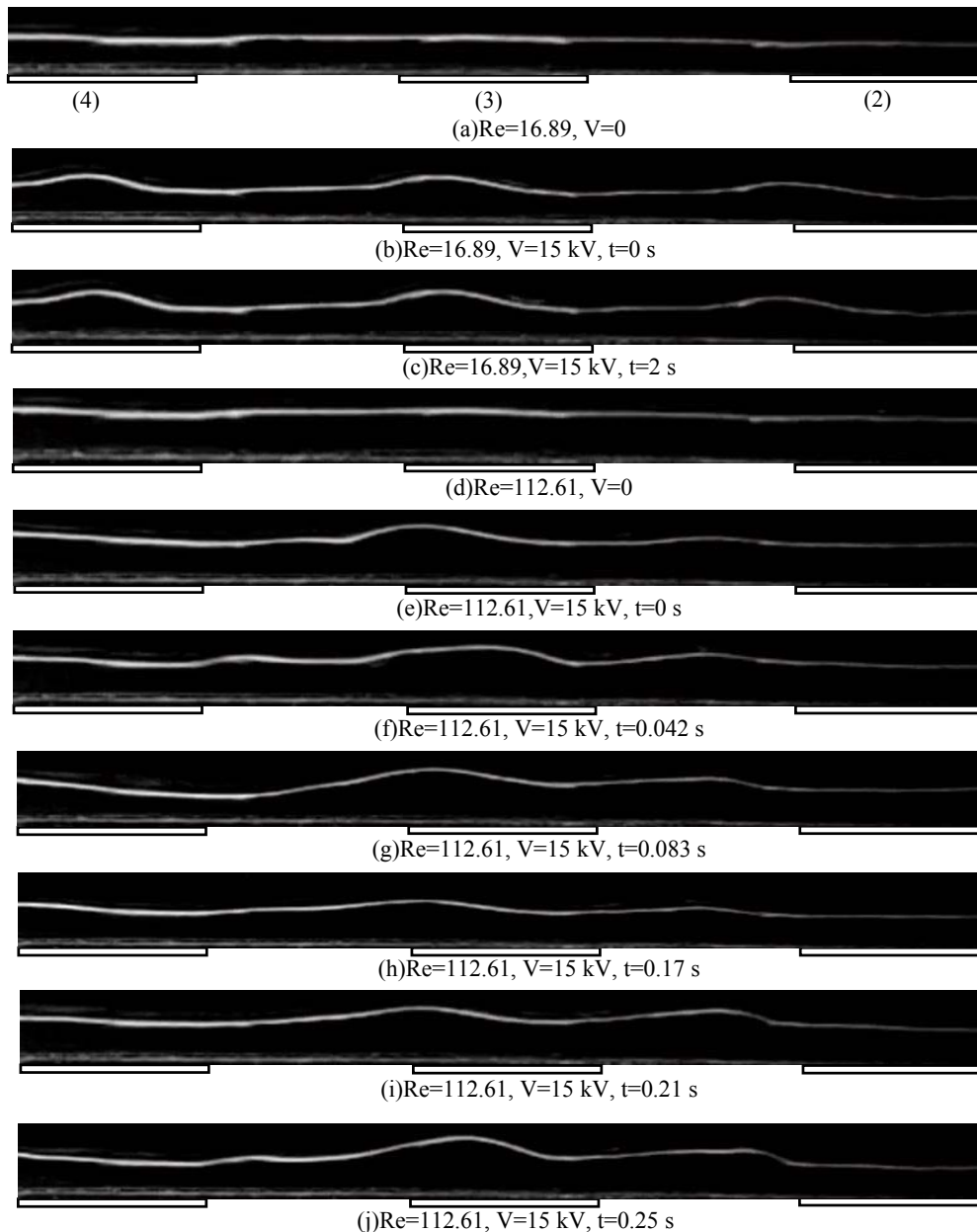


Fig. 6. Waves profile of falling film for $\theta=30^\circ$

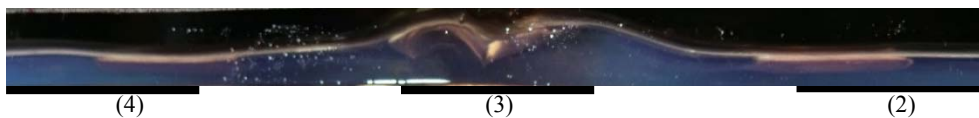
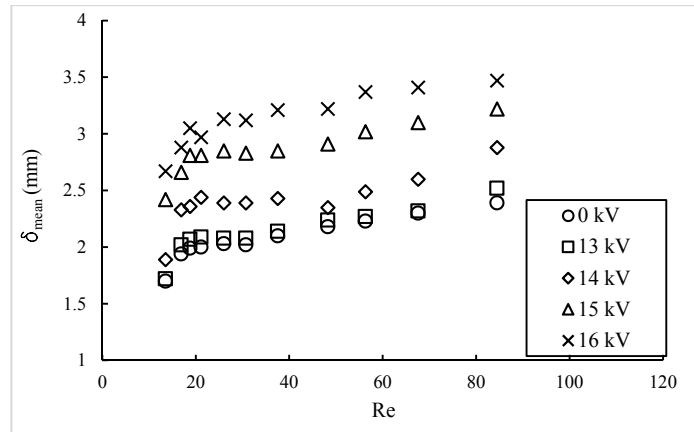


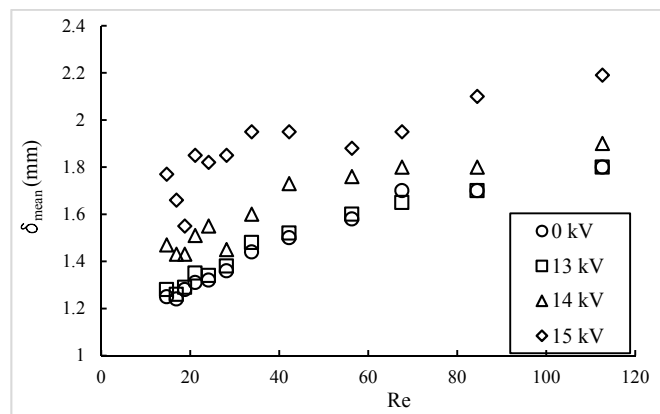
Fig. 7. Discharge phenomena from third HV wire electrode to film interface at $Re=84$, $\theta=15^\circ$ and $V=16.5$ kV

Figure 8 presents how the mean film thickness is varied in terms of Reynolds number for different inclinations and voltages when EHD is imposed. It is concluded that non-electrified film thickness decreases by increasing the inclination angle (Brauner and Maron 1982) and in all inclinations, EHD phenomena increase the mean film thickness by generating the large waves on the film surface because of preserving a volume of fluid inside the waves. When the voltage and inclination angle are increased, the mean film thickness slightly decreases.

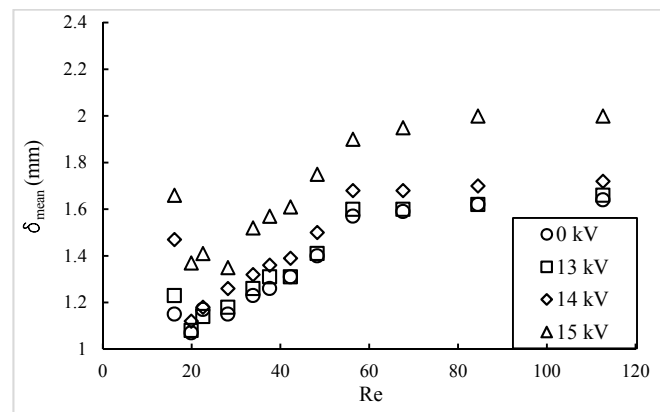
It can be seen that the electric field effect strengthened by increasing the applied voltage in most of Reynolds numbers. In larger inclinations, the higher momentum of the natural waves than EHD generated waves prevents from holding the volume of fluid on the ground electrodes and leads to decrease the wave height. On the other hand, decreasing the mean film thickness by increasing the inclination, the air gap between HV wire and the ground electrode will increase.



(a)



(b)



(c)

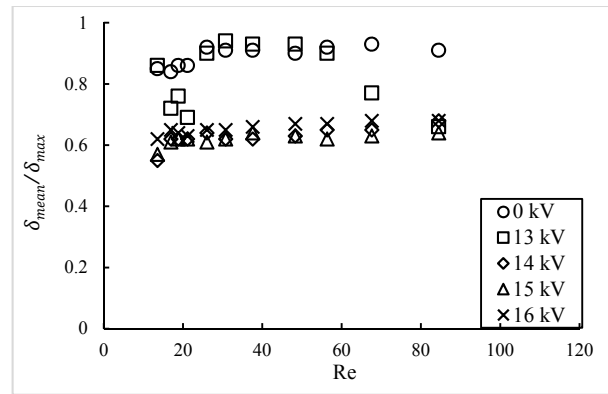
Fig. 8. Mean film thickness for different voltages versus Re number (a) $\theta=15^\circ$, (b) $\theta=30^\circ$ and (c) $\theta=45^\circ$

The air gap influences the momentum transfer between ionized air molecules and the liquid/air interface. With a close look at Fig. 8, it can be found that the slope of the mean film thickness curve as a function of Reynolds number becomes steeper by increasing the inclination for voltages.

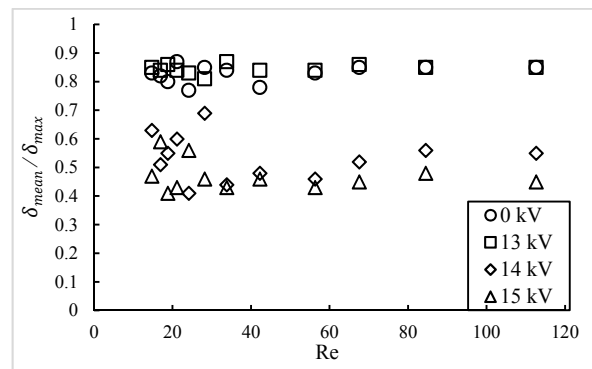
In Fig. 9, the ratio of mean film thickness to maximum film thickness has been figured in terms of Reynolds number for three different inclination

angles. The probability of 5% or less has been used to determine the maximum film thickness.

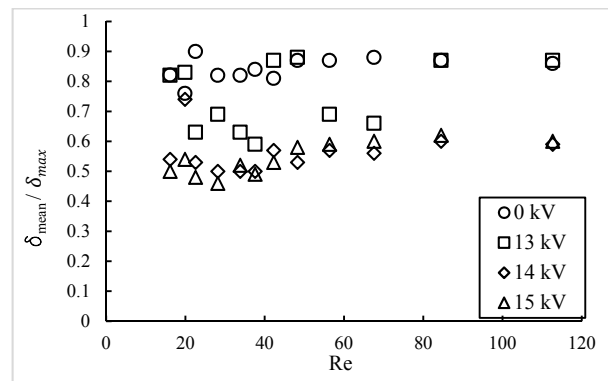
This ratio can be used as a criterion for measuring the large waves' effect on the mean film thickness (Moran 1997). As mentioned before, EHD phenomenon increases the maximum wave thickness like the mean film thickness for all the Re numbers and the inclination angles. The large waves play a significant role in increasing the mean



(a)



(b)



(c)

Fig. 9. Ratio of mean to maximum film thickness (a) $\theta=15^\circ$, (b) $\theta=30^\circ$ and (c) $\theta=45^\circ$

and maximum values. However, the increase rate of the maximum film thickness with the Reynolds number and inclination angle is greater than that of the mean data. In addition, the maximum film thickness increases as a function of the voltage. Figure 9 shows that low voltages have a little influence on the flow maximum thickness and $\delta_{mean}/\delta_{max}$ (special for low inclination angles), while the effect of higher voltages on large waves is significant and leads to be lesser value of $\delta_{mean}/\delta_{max}$ for all the cases.

Additional information can be concluded from Fig. 9. The mean height of the waves is similar in low

angles, and the rise of the voltage does not have significant effect. On the other hand, mean thickness of the waves will become lower than maximum thickness in angles higher than 15° and by the increase of the voltage greater than 13 kV, the large wave is formed and is intensified by the increase of Reynolds number.

In order to investigate probability density function (PDF) variation, the film thickness with $\Delta\delta = 0.1 \text{ mm}$ interval is used to calculate the substrate film thickness in order to study the film waviness at different Reynolds numbers and voltages. The peak of PDF curve is defined as the substrate thickness

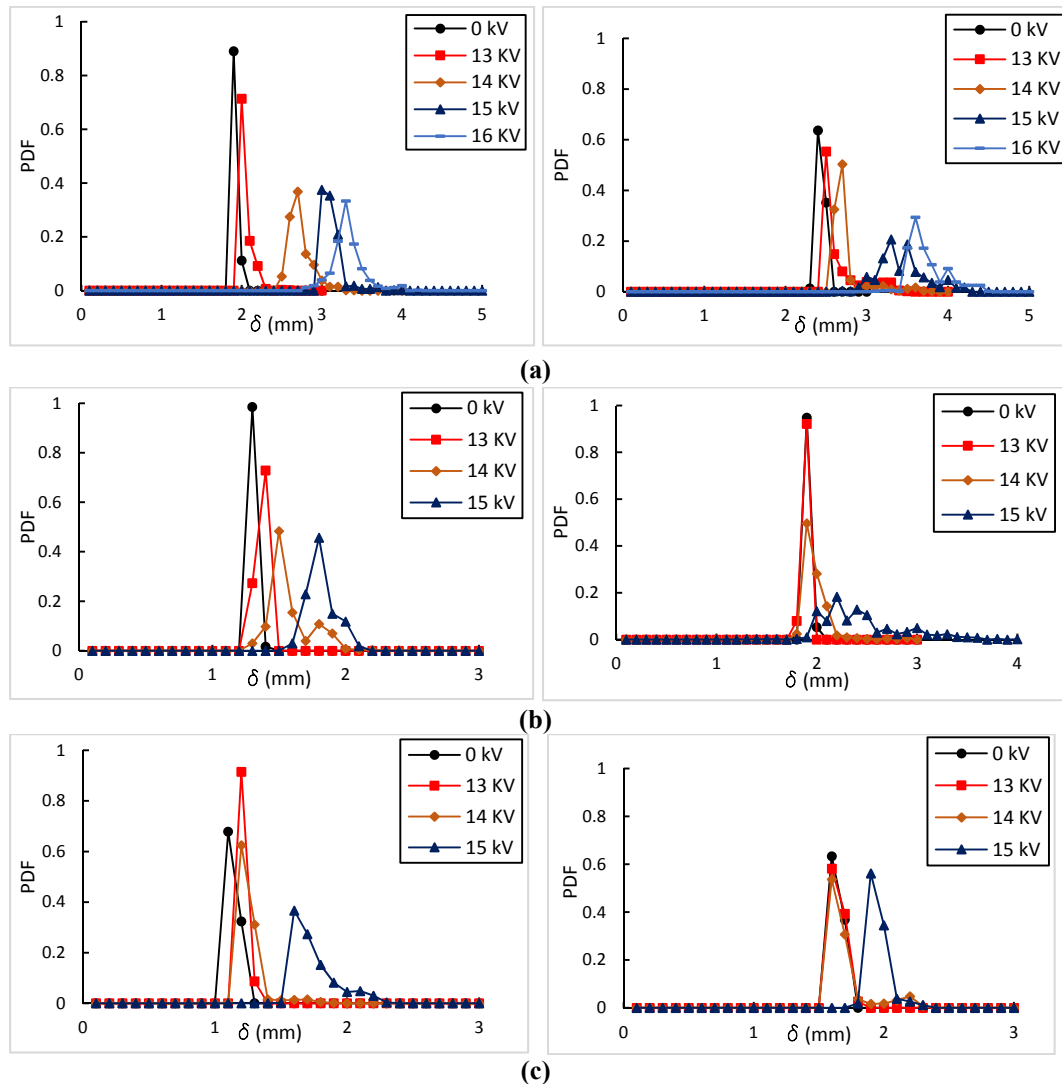


Fig. 10. Probability density distribution of local film thickness for (a) $\theta=15^\circ$, (b) $\theta=30^\circ$ and (c) $\theta=45^\circ$ ($Re = 16$ (left) and $Re = 84$ (right))

which is the bound of the most probable film thickness (Chu and Dukler 1974), (Chu and Dukler 1975). In condensers or other falling film heat exchangers, this thickness plays the role of the main thermal resistance against the heat transfer between wall and gas stream. In the present study, probability density function has been calculated at distance 226 mm from the film entry (the middle of the 3rd electrode) in order to study the effect of EHD phenomenon.

Figure 10 displays probability density distribution of wave peaks at low and high Reynolds numbers for three inclination angles. It can be seen that without the electric field, PDF distribution has a sharp peak at about the mean thickness value, but remains close to zero for greater thickness values, indicating the existence of few waves. The substrate thickness of the film increases by Re number for all inclinations, as shown in Fig. 10. By applying the electric field, the range of fluctuations of thickness extends by decreasing inclination angle and this expansion is toward higher thickness. These data confirm the fact that the gravitational waves along the inclined surface

reduce the waviness of the film; therefore, the effect of voltage on the substrate thickness reduces by the increase of inclination. At high Re numbers, the interaction between gravitational waves and EHD waves reduces strongly the waviness of the interface for high inclination because of accelerating the liquid falling film. Some general trends from Fig. 10 can be noted as follows:

- (a) When the voltage increases, the substrate film thickness tends to rise.
- (b) The degree of waviness increases at high voltages.
- (c) The peak value of the probability density function decreases with increasing Reynolds number and voltage for most cases.

Although by application of EHD, the substrate thickness increases and prevents the penetration of weak disturbances to the inner layer of the film but the waviness of the falling film also increases, which can augment the heat transfer rate between the liquid film

and ambient air by increasing the film surface area.

It was previously reported that the wavy structure of falling films enhances heat/mass transfer across the liquid interface. Therefore, it may be interesting to investigate the frequency with which these waves occur (Moran 1997). The wave frequency determined by the power spectral density function, have been presented in Fig. 11 in terms of Reynolds number at different inclination angles with and without the electric field. All the calculated spectral density functions exhibit a very noticeable maximum within the frequency range 2 to 6 Hz. This frequency characterizes the large waves and looks not to be dependent upon the Reynolds number (Karapantsios, Paras, and Karabelas 1989).

Figure 11 shows that the wave frequency is nearly constant over the range $Re \approx 10-120$ without EHD at 15° . By increasing the inclination angle, the wave frequency tends to increase with and then decrease without the electric field. It is evident that by increasing the voltage, the wave frequency slightly increases and then decreases with Re and inclination angle because of the distance between the available waves at the free surface. In low Re , these waves are

far enough apart, and they do not go across each other; therefore, the velocity of the waves and their frequency will increase by exerting the EHD on falling film. Whereas in high Reynolds, this tendency varies, and they can strongly influence each other due to the shorter wavelength of the waves and integrated into one wave with larger wavelength. In this case, the available number of the waves on the free surface will decrease, which leads to lower frequencies (Sobhani *et al.* 2015).

In order to evaluate the wave velocity, the statistical cross-covariance analysis has been performed to estimate the wave migration time for non-electrified falling films. In the case of electrified falling film, if the falling film shape was noticeably deformed, the cross-covariance method can't estimate the wave velocity accurately as mentioned by (Brauner and Maron 1982). It is observed that at low voltages, stable pattern of the wave is formed at the interface; therefore, the cross-covariance method can be used to determine the velocity of the waves in this case. For higher voltages, the waves on the falling film deformed significantly, the wave velocity has been evaluated by the direct data inspection method (Kostoglou, Samaras, and Karpantsios 2009).

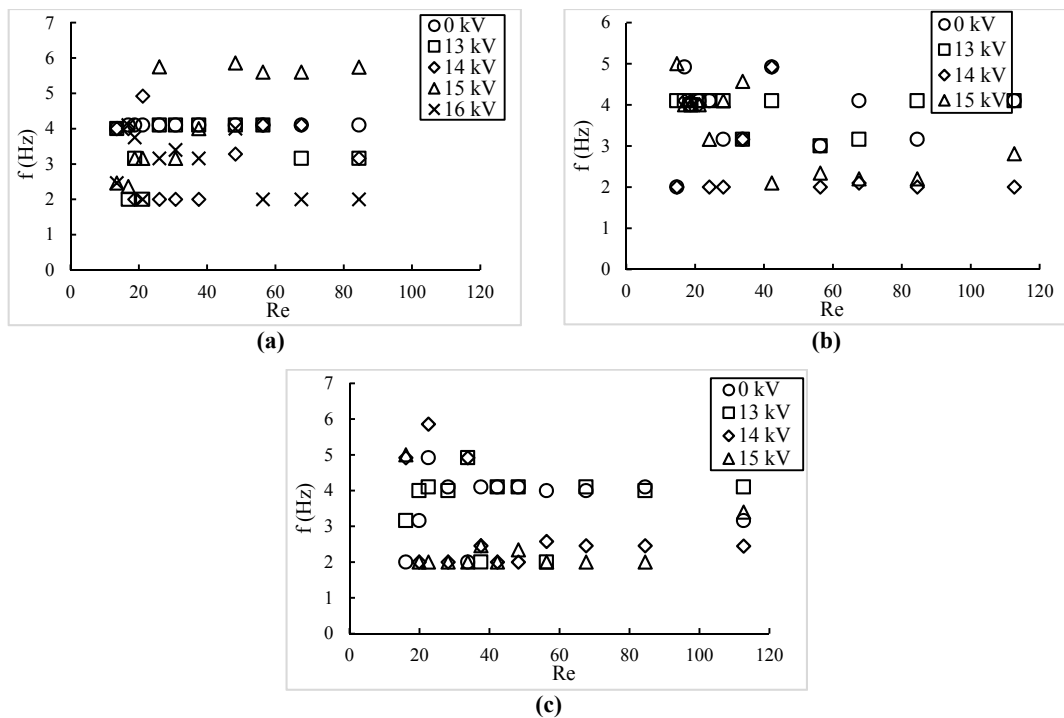


Fig. 11. Wave frequency for different voltages versus Re number (a) $\theta=15^\circ$, (b) $\theta=30^\circ$ and (c) $\theta=45^\circ$

Figure 12 suggests that the waves accelerate by the increase of the voltage and degree of inclination. The effect of voltages on the wave velocity is not significant in low Reynolds numbers, but it will be considerable for higher Reynolds. The increase of the film thickness fluctuation and the amplitude of the generated waves by the electric field (Figs. 8, 9 and 10) cause to the increase of the wave velocity with respect to the non-electrified one.

The standard deviation of local film thickness can be used to measure the scattering of film thickness about its mean value (Karapantsios, Paras, and Karabelas 1989). Figure 13 shows the influence of Reynolds number, inclination angle, and voltage on the standard deviation which appears to be nearly constant (around 0.02) throughout the Reynolds range for the non-electrified falling film. When the EHD is imposed on the falling film, the following points can be extracted:

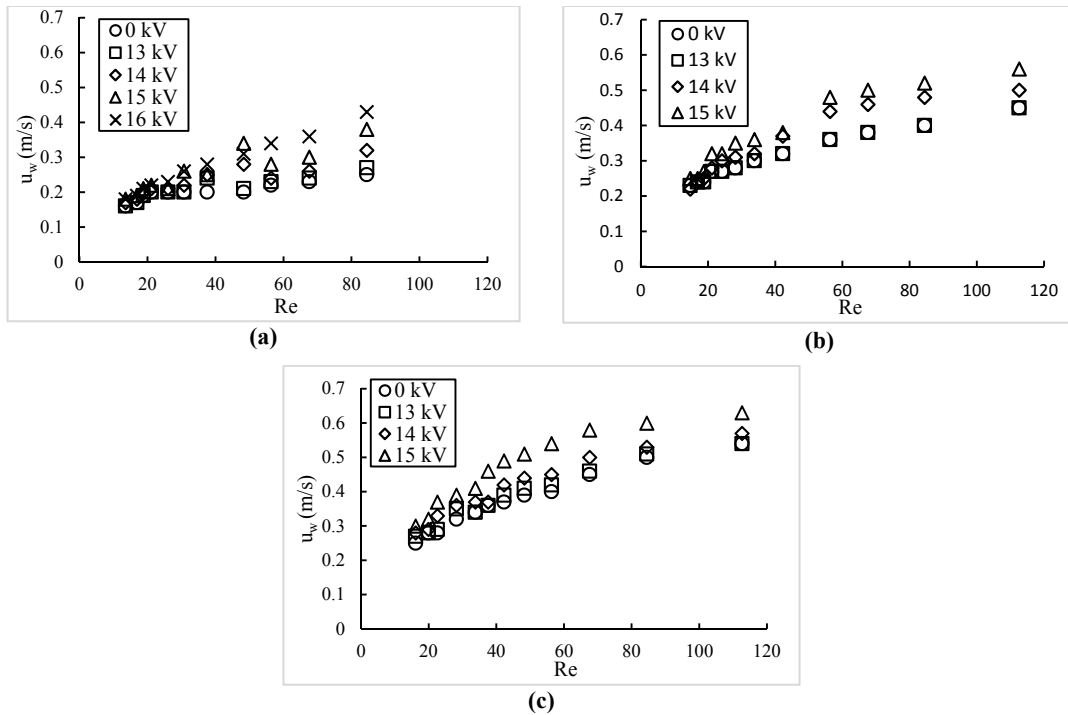


Fig. 12. Wave velocities versus Reynolds number for different inclination angles and voltages (a) $\theta=15^\circ$, (b) $\theta=30^\circ$ and (c) $\theta=45^\circ$

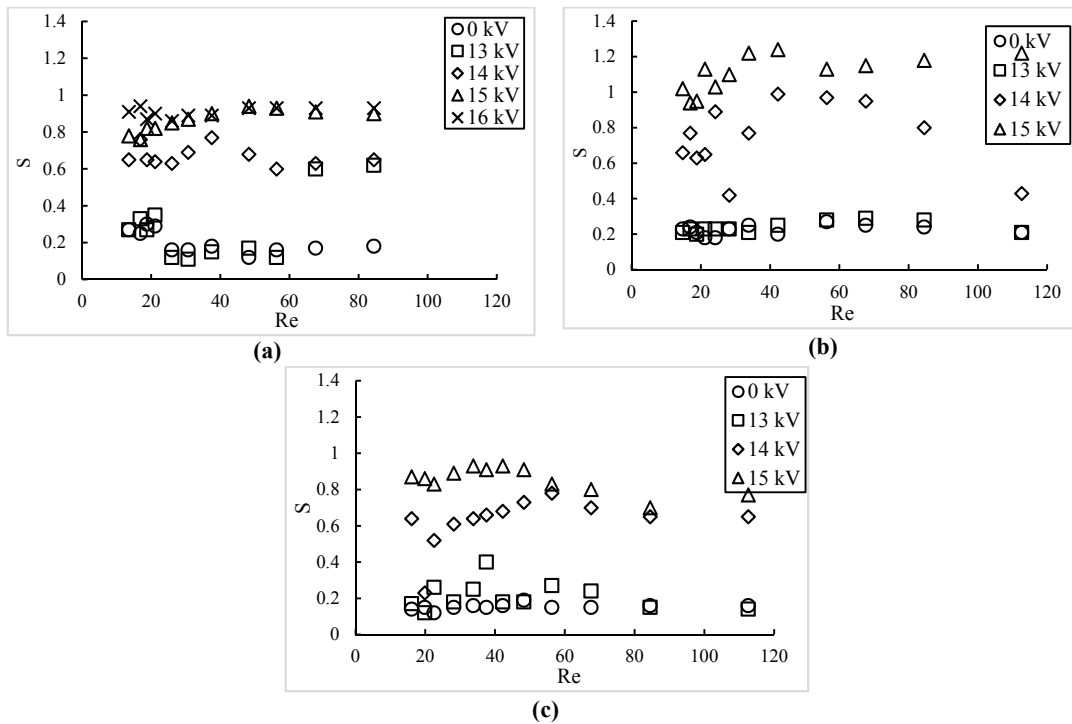


Fig. 13. Effect of Reynolds number on the standard deviation of film thickness for each inclination angle (a) $\theta=15^\circ$, (b) $\theta=30^\circ$ and (c) $\theta=45^\circ$

(1) By applying EHD, the wavy behavior of falling film intensified and standard deviation increases.

(2) For a high degree of inclination, the standard deviation significantly increases.

It is interesting that a substantial increase of the

standard deviation takes place up to a special Re for each inclination, then, the standard deviation tends to decrease.

6. CONCLUSION

A developing laminar falling film has been

investigated experimentally for cases, which include a unique EHD application and compare with tests without electric fields. This new EHD configuration imposed on a dielectric liquid by some pairs of the HV-wires and grounded-plate electrodes in the Reynolds number range of 10-120. This mechanism requires no electrical contact with the fluid as an advantage; therefore, we can use the wide range of liquids with low conductivity. In this phenomenon, the electric field induces the free charges on the liquid interface and due to the interaction between electrical and gravitational forces; the significant surface waves appear on the liquid free surface and enhance the heat/mass transfer rate. Three different inclination angles have been selected for this study, and the transformer oil has been selected because of its favorable electrical properties. The results indicate that EHD phenomenon increases the mean film thickness and substrate thickness for all Reynolds numbers. Furthermore, applying the electric field on the film accelerates the waves by increasing the voltage but the wave frequency fluctuates by around 4 Hz in different voltages. It is observed that the wave frequency increases by voltage but reduces for high voltages at low inclination. When the inclination increases, this effect becomes reverse. The standard deviation of local film thickness tends to increase for all Reynolds numbers by applying the electric field, which implies that the wavy behavior of film is intensified in the presence of EHD. Finally, it is concluded that the proposed EHD pattern requires more experimental and computational studies for accurate judgment about its effectiveness on the heat/mass transfer augmentation, since this investigation has been done based on the hydrodynamic behavior of waves.

REFERENCES

- Ambrosini, W. *et al.* (1999). Experimental Investigation on Wave Velocity in a Falling Film. In *2-Nd Int. Symp. Two-Phase Flow Modelling and Experimentation*, 23–26.
- Bobylev, A., V. Guzanov, A. Kvon, and S. Kharlamov (2016). Characteristics of Film Flow during Transition to Three- Dimensional Wave Regimes. *Journal of Physics: Conference Series* 754, 1–6.
- Brauer, H. (1956). Strömung Und Wärmeübergang Bei Rieselfilmen. *VDIForschungsheft 457B* 22, 1–40.
- Brauner, N., and Moalem Maron D. (1982). Characteristics of Inclined Thin Films, Waviness and the Associated Mass Transfer. *International Journal of Heat and Mass Transfer* 25(1), 99–110.
- Charogiannis, A., S. A. Jae, and C. N. Markides (2015). A Simultaneous Planar Laser-Induced Fluorescence, Particle Image Velocimetry and Particle Tracking Velocimetry Technique for the Investigation of Thin Liquid-Film Flows. *Experimental Thermal and Fluid Science* 68, 516–36.
- Chirkov, V. A. (2013). *Influence of Charge Formation Mechanism on the Structure of Electrohydrodynamic Flow in Highly Non-Uniform Electric Field*. Saint Petersburg State University.
- Chu, K. J., and A. E. Dukler (1974). Statistical Characteristics of Thin, Wavy Films Part 2. Studies of the Substrate and Its Wave Structure. *AIChE Journal* 20(4), 695–706.
- Chu, K. J., and A. E. Dukler (1975). Statistical Characteristics of Thin , Wavy Films. Part 3: Structure of the Large Waves and Their Resistance to Gas Flow. *AICHE J.* 21(3), 583–93.
- Damianidis, C., T. G. Karayiannis, and R. K. *et al.* Al-Dadah (1992). EHD Boiling Enhancement in Shell-and-Tube Evaporators and Its Application in Refrigeration. In *ASHRAE*.
- Drosos, E. I. P., S. V. Paras, and A. J. Karabelas (2004). Characteristics of Developing Free Falling Films at Intermediate Reynolds and High Kapitza Numbers.” *International Journal of Multiphase Flow* 30(7-8 SPEC. ISS.), 853–76.
- Gharraei, R. (2011). *Hydrodynamic Investigation of Falling Film in the Presence of Electric Field*. University of Tabriz.
- Gharraei, R., M. Hemayatkhah, S. Baheri Islami, and E. Esmaeilzadeh (2015). An Experimental Investigation on the Developing Wavy Falling Film in the Presence of Electrohydrodynamic Conduction Phenomenon. *Experimental Thermal and Fluid Science* 60(JANUARY 2015), 35–44.
- Gonzalez, A., and A. Castellanos (1996). Nonlinear Electrohydrodynamic Waves on Films Falling down an Inclined Plane. *Physical Review E* 53(4), 3573–78.
- Jackson, M. L. (1955). Liquid Films in Viscous Flow. *AICHE J.* 1, 231–40.
- Jones, L. O., and S. Whitaker (1966). An Experimental Study of Falling Liquid Films. *AICHE J.* 12, 525–29.
- Karami, R *et al.* (2012). An Experimental Study of the Effect of High Electric Field on Mass Transfer Enhancement. *Journal of Petroleum Science and Technology* 2(2), 40–49.
- Karapantsios, T. D., S. V. Paras, and A. J. Karabelas. 1989. “Statistical Characteristics of Free Falling Films at High Reynolds Numbers.” *International Journal of Multiphase Flow* 15(1): 1–21.
- Kostoglou, M., K. Samaras, and T. D. Karpantsios (2009). “Large Wave Characteristics and Their Downstream Evolution at High Reynolds Number Falling Films. *AICHE J.* 56(1), 11–23.
- Laohalertdech, S. , P. Naphon, and S. Wongwises (2007). A Review of Electrohydrodynamic Enhancement of Heat Transfer. *Renewable and Sustainable Energy Reviews* 11(5), 858–76.
- Léal, L. *et al.* (2013). An Overview of Heat

- Transfer Enhancement Methods and New Perspectives: Focus on Active Methods Using Electroactive Materials. *International Journal of Heat and Mass Transfer* 61(1), 505–24.
- Lel, V. V., F. Al-Sibai, A. Leefken, and U. Renz (2005). Local Thickness and Wave Velocity Measurement of Wavy Films with a Chromatic Confocal Imaging Method and a Fluorescence Intensity Technique. *Experiments in Fluids* 39(5), 856–64.
- Martin, M., T. Defraeye, D. Derome, and J. Carmeliet (2015). A Film Flow Model for Analysing Gravity-Driven, Thin Wavy Fluid Films. *International Journal of Multiphase Flow* 73, 207–16.
- Melcher, J. R. (1966). Traveling Wave Induced Electroconvection. *Physics of Fluids* 9(8), 1548–55.
- Miyara, A. (1999). Numerical Analysis on Flow Dynamics and Heat Transfer of Falling Liquid Films with Interfacial Waves. *Heat and Mass Transfer* 35(4), 298–306.
- Moffat, R. J. (1988). Describing the Uncertainties in Experimental Results. *Experimental Thermal and Fluid Science* 1, 3–17.
- Molki, M., M. Ohadi, and L. W. Da Silva (2002). EHD-Assisted Condensation OF Refrigerant R-134a on Tube Bundle. In *8th AIAA/ASME Joint Thermophysics and Heat Transfer Conference*, 1–8.
- Moran, K. (1997). *Experimental Study of Laminar Liquid Films Falling on an Inclined Plate*. University of Toronto.
- Moran, K., J. Inumaru, and M. Kawaji (2002). Instantaneous Hydrodynamics of a Laminar Wavy Liquid Film. *International Journal of Multiphase Flow* 28(5), 731–55.
- Nourdanesh, N., and E. Esmaeilzadeh (2013). Experimental Study of Heat Transfer Enhancement in Electrohydrodynamic Conduction Pumping of Liquid Film Using Flush Electrodes. *Applied Thermal Engineering* 50(1), 327–33.
- Nusselt, W. (1916). Die Oberflächenkondensation Des Wasserdampfes. *VDI-Zs* 60, 541.
- Ogata, J., and A. Yabe. (1993). Augmentation of Boiling Heat Transfer by Utilizing the EHD Effect-EHD Behaviour of Boiling Bubbles and Heat Transfer Characteristics. *International Journal of Heat and Mass Transfer* 36(3), 783–91.
- Ohyama, R., A. Watson, and J. S. Chang (2001). Electrical Current Conduction and Electrohydrodynamically Induced Fluid Flow in an AW Type EHD Pump. *Journal of Electrostatics* 53(2), 147–58.
- Paillat, T., and G. Touchard (2009). Electrical Charges and Liquids Motion. *Journal of Electrostatics* 67(2-3), 326–34.
- Portalski, S. (1964). Velocities in Film Flow of Liquids on Vertical Plates. *Chemical Engineering Science* 19(8), 575–82.
- Raghavan, R. V. *et al.* (2009). Electrokinetic Actuation of Low Conductivity Dielectric Liquids. *Sensors and Actuators, B: Chemical* 140(1), 287–94.
- Samanta, A. (2013). Shear Wave Instability for Electrified Falling Films. *Physical Review E* 88(5), 1–7.
- Seyed-Yagoobi, J., and J. E. Bryan (1999). Enhancement of Heat Transfer and Mass Transport in Single-Phase and Two-Phase Flows with Electrohydrodynamics. *Advances in Heat Transfer* 33, 95–186.
- Sobhani, A., Sh. Nasirivatan, R. Gharraei, and E. Esmaeilzadeh (2015). Experimental Investigation of Fully Developed Falling Film Flow in the Presence of Conduction Pumps. *Journal of Electrostatics* 73, 71–79.
- Tareev, B. (1975). *Physics of Dielectric Materials*. Mir.
- Tseluiko, D., M. G. Blyth, D. T. Papageorgiou, and J. M. Vanden-Broeck (2010). Electrified Falling-Film Flow over Topography in the Presence of a Finite Electrode. *Journal of Engineering Mathematics* 68(3), 339–53.
- Tseluiko, D., and D. T. Papageorgiou (2006). Wave Evolution on Electrified Falling Films. *Journal of Fluid Mechanics* 556, 361–86.
- Wang, P., P. L. Lewin, D. J. Swaffield, and G. Chen (2009). Electric Field Effects on Boiling Heat Transfer of Liquid Nitrogen. *Cryogenics* 49(8), 379–89.
- Wray, A. W., O. Matar, and D. T. Papageorgiou (2012). Non-Linear Waves in Electrified Viscous Film Flow down a Vertical Cylinder. *Journal of applied mathematics* 77, 430–40.